Environmental Science and Pollution Research (2022) 29:84006–84018
https://doi.org/10.1007/s11356-022-21701-0

RESEARCH ARTICLE

Effect of ternary polymer composites of macroporous adsorbents on adsorption properties for heavy metal removal from aqueous solution

Methus Charoenchai[1] · **Siree Tangbunsuk**[1]

Received: 24 February 2022 / Accepted: 23 June 2022 / Published online: 1 July 2022

Abstract
This research is focused on the preparation of macroporous poly(vinyl alcohol) (PVA)/chitosan (CS)/Al_2O_3 adsorbents for removal of residual metal ions from wastewater. The PVA/CS/Al_2O_3 adsorbents were characterized by X-ray diffraction (XRD), Brunauer–Emmett–Teller (BET), and energy dispersive X-ray (EDX) techniques to confirm that all compositions were incorporated into the PVA/CS/Al_2O_3 adsorbents without chemical modification. Furthermore, a comparison of the properties of the PVA/CS/Al_2O_3 adsorbents suggested that PVA/CS/0.50Al_2O_3 was the most suitable sample for adsorption study. The adsorption properties of PVA/CS/0.50Al_2O_3 for the removal of metal ions such as Pb^{2+}, Cu^{2+}, Zn^{2+}, and Ni^{2+} in aqueous solution adsorbents in both single and quaternary systems were investigated. The results show that the adsorption selectivity of the PVA/CS/0.50Al_2O_3 adsorbent for these metal ions was provided in the following order: $Pb^{2+} > Cu^{2+} > Zn^{2+} > Ni^{2+}$. The adsorption isotherm was studied by equilibrium data obtained from batch experiments. It was found that the Freundlich isotherm model was suitable for explaining the adsorption process. Adsorption kinetics were studied, which indicated that the adsorption of Pb^{2+}, Cu^{2+}, and Zn^{2+} followed a pseudo-second-order kinetic model, while the adsorption of Ni^{2+} followed a pseudo-first-order kinetic model. In addition, adsorption–desorption cycles were studied to prove the reusability of PVA/CS/0.50Al_2O_3 adsorbents. The PVA/CS/0.50Al_2O_3 adsorbents were able to be regenerated and reused. In a continuous adsorption process, a column experiment was simulated in laboratory. The results showed that Cu^{2+} was the most selective for a fixed-bed column. Thus, PVA/CS/0.50Al_2O_3 adsorbents could be potential used for toxic metal ion removal from wastewater, in both batch and fixed-bed continuous-flow columns.

Keywords Composite adsorbents · Metal pollutants · Chitosan · Poly(vinyl alcohol) · Alumina

Introduction

Recently, water pollution by heavy metals has been increasing worldwide. Data from the period 1972–2017 shows that almost all of the heavy metals Cd, Pb, Cu, Cr, Hg, Zn, Ni, Al, Fe, Mn, As, and Co were present in global river and lake water in higher concentrations than the published threshold limits suggested as standards by World Health Organization (WHO). This is an important environmental problem all over the world due to rapid growth of industry, and the increase in human population and agricultural activities (Zhou et al. 2020). This leads to life-threatening diseases. Even low concentration of toxic heavy metals in water sources can cause serious health problems, through the accumulation in living tissues over time, leading to many diseases and disorders (Futalan et al. 2011; Mishra and Patel 2009). Various toxic metal ions such as Pb, Cu, Zn, and Ni are accumulated in the consumer's body, which leads to genetic changes and cancer (Sharma et al. 2009). These pollutants are unable to be decomposed by natural processes. Thus, many suitable technologies are being developed for metal removal in the effort to solve these problems.

There are many kinds of technology for heavy metal removal. For example, techniques including ion exchange, reverse osmosis, electrolytic removal, reduction,

Responsible Editor: Tito Roberto Cadaval Jr

✉ Siree Tangbunsuk
siree.t@ku.ac.th

Methus Charoenchai
methus.ch@ku.th

[1] Department of Chemistry, Faculty of Science, Kasetsart University, Bangkok 10900, Thailand

precipitation, flocculation, membrane filtration, and adsorption have all been developed. However, some of these technologies (such as ion exchange, reverse osmosis, electrolytic removal, reduction, precipitation, flocculation, and membrane filtration) are costly in their operation and equipment, have high energy consumption, and are inefficiency techniques that cause toxic metal residues (Sharma et al. 2009). Adsorption is an interesting technique for heavy metal removal because this technique offers flexibility in design and operation, and it can generate treated effluents of high quality. Furthermore, it is an eco-friendly technique, with minimal energy consumption, and the adsorbents can be regenerated by simple desorption methods due to the reversible nature of most adsorption processes. Many desorption processes have low maintenance costs, and high efficiency and ease of operation (Hua et al. 2012). Thus, the adsorption process has become the first choice for heavy metal removal from wastewater.

Previously, many adsorbents used to perform this method consisted of chemicals prepared under harsh conditions, such as high pressure and temperature. This required higher energy inputs and therefore higher costs. There are many types of materials used as adsorbents, such as activated carbon, fly-ash, zeolite, earth clay, sphagnum moss peat, chitosan, and alumina. In addition, a combination of these materials could exhibit effective adsorption characteristics. The development of adsorbents using an economically simple method and inexpensive available materials would be a significant achievement.

The biodegradable polymers, such as poly(vinyl alcohol) (PVA) and chitosan (CS), are potential candidates for use as adsorbents due to their outstanding properties, such as adsorption affinity, high durability, high chemical stability and biocompatibility, low cost, and minimal environmental impact. Often, one material used on its own can have low efficiency. For example, there may be difficulty in operation or limitations in metal adsorption. Thus, many investigations reported in the literature have synthesized and studied binary composite adsorbents to enhance the adsorption properties. For example, the PVA/CS adsorbents have been studied, exhibiting affinities for metal ion removal in the following order: $Cu^{2+} > Pb^{2+} > Cd^{2+} > Zn^{2+}$ (Li et al. 2011).

Alumina or aluminum oxide (Al_2O_3) is widely used in many applications, such as microelectronics, catalyst support, mechanical structure, selective membrane application, and wastewater treatment. Various investigations have suggested that Al_2O_3 has the potential to remove metal ions such as Pb^{2+}, Cr^{2+}, Cu^{2+}, Cd^{2+}, Ni^{2+}, and Hg^{2+} from synthetic solutions and wastewater from industry (Hua et al. 2012; Rahmani et al. 2010). In addition, Al_2O_3 particles were synthesized by a simple sol–gel method, which allowed the control of particle size. A small particle size increases the surface area, improving the effectiveness of the adsorption process due to the increased amount of binding sites (Rahmani et al. 2010).

This research aimed to fabricate novel composite adsorbents based on biodegradable polymeric materials, polyvinyl alcohol (PVA), and chitosan (CS), with incorporated alumina (Al_2O_3), in order to improve the adsorption properties of metal ion removal. The PVA/CS/Al_2O_3 composite adsorbents would be expected to display improved adsorption efficiency, as there is an increase in the surface area proportional to the number of active sites. In addition, these materials would be expected to have biodegradable properties, as only small amounts of alumina (0.75 g and 1.5 g, for the mass ratios of 0.25 and 0.50, respectively) was used to synthesize the adsorbents. These adsorbents are eco-friendly in nature, reusable, and can be efficiently regenerated.

Experimental

Materials and methods

Poly(vinyl alcohol) (PVA) (molecular weight ~ 50,000–85,000 g/mol), chitosan (CS) (molecular weight ~ 100,000–300,000 g/mol), and sodium alginate (Na-Alg) were purchased from Arcos, Belgium. Calcium carbonate ($CaCO_3$) and aluminum sulfate ($Al_2(SO_4)_3$) used in this work were acquired from Ajax Finechem Pty. Ltd., Australia. Calcium chloride ($CaCl_2$) and boric acid (H_3BO_3) were obtained from Carlo Erba Reagents S.A.S., France. Ammonium hydroxide (NH_4OH), hydrochloric acid (HCl), lead (II) nitrate ($Pb(NO_3)_2$), and nickel (II) nitrate hexahydrate ($Ni(NO_3)_2{\cdot}6H_2O$) were received from Qrec, New Zealand. Copper (II) nitrate tetrahydrate ($Cu(NO_3)_2{\cdot}4H_2O$) and zinc (II) nitrate hexahydrate ($Zn(NO_3)_2{\cdot}6H_2O$) were purchased from Loba Chemie Pvt. Ltd., India. These chemicals were of analytical grade and used as received without further purification.

Preparation of aluminum oxide particles (Al_2O_3)

In a typical procedure, Al_2O_3 particles were synthesized by a sol–gel method with $Al_2(SO_4)_3$ and NH_4OH solutions (Sharma et al. 2008). One hundred milliliters of a 0.5 M solution of $Al_2(SO_4)_3$ was prepared by dissolving $Al_2(SO_4)_3$ powder in distilled water and then slowly adding NH_4OH to form precipitates. These precipitates were separated by centrifugation at 10,000 rpm for 10 min and then washed with distilled water. The precipitates were then collected and dried at 80 °C for 24 h. In order to obtain the appropriate particle size, the resulting particles were milled into a small powder. Then, the particles were calcined at 1100 °C for 1 h to obtain alumina powder. Finally, this powder was milled again by ball mill and sieved (45 μm) after calcinations, to obtain the small Al_2O_3 particles.

Preparation of PVA/CS/Al_2O_3 adsorbents

The PVA/CS/Al_2O_3 adsorbents were prepared through a simple reaction. PVA (6 g), Na-Alg (1.3 g), and $CaCO_3$ (10 g) were dissolved in 150 mL of distilled water and the mixture was heated at 90 °C for 2 h. Then, CS (7.5 g) and Al_2O_3 (0, 0.75, and 1.5 g for the mass ratios of 0, 0.25, and 0.50, respectively) were added to the mixture and stirred continuously for 6 h at 90 °C. The mixture was slowly dropped by syringe into a 3 wt% $CaCl_2$-saturated H_3BO_3 solution to create composite adsorbents and then carefully stirred for 48 h to become stable. HCl (1 M) was then added until no bubbles were being generated, to form macroreticular adsorbents. The adsorbents were washed with distilled water several times to become neutral and then dried at room temperature to obtain porous PVA/CS/Al_2O_3 adsorbents.

Characterization

X-ray diffraction (XRD) patterns were observed by Bruker D8 Advance X-ray diffractometer, with a Cu-K_α, X-ray source ($\lambda = 1.54$ Å) at a scan rate of 0.05°/s in the 2θ range from 5° to 80°, in order to investigate the composition of all samples and confirm that Al_2O_3 particles were incorporated into the PVA/CS/Al_2O_3 adsorbents.

Brunauer–Emmett–Teller surface analysis (BET) was introduced to investigate the specific surface area, pore volume, and pore diameter of the prepared adsorbents. The samples were analyzed using a Micromeritics 3Flex Surface Characterization Analyzer. All of the synthesized adsorbents were adsorbed with N_2 in an analysis bath at − 196 °C and desorbed at 80 °C overnight.

The morphology of PVA/CS/Al_2O_3 adsorbents was observed using FEI Quanta 450 scanning electron microscope (SEM) with a voltage of 15 kV. This Quanta SEM was equipped with energy dispersive X-ray spectroscopy (EDX) to evaluate the elemental composition of the synthesized samples. The samples were held on a specimen stub with carbon tape adhesive.

Fourier-transform infrared (FTIR) analysis was performed to study the adsorption mechanism of PVA/CS/0.50Al_2O_3, before and after adsorption, by using a Spectrum Two PerkinElmer equipped with a diamond attenuated total reflection (ATR) device at room temperature and a scanning range of 4000–400 cm^{-1}.

Adsorption experiments for a single system

The adsorption experiments began with metal stock solutions. The stock solutions of metal ions (Pb^{2+}, Cu^{2+}, Zn^{2+}, and Ni^{2+}) with concentrations of 1000 mg/L were prepared by dissolving the appropriate metal nitrate in deionized water and then diluted to prepare working solutions in the range of 100–500 mg/L. Adsorbents (0.1 g) were added to 50 mL of metal solution. All of the batch experiments were performed in 250 mL conical flasks with stoppers and these flasks were shaken in a temperature-controlled shaker at 100 rpm, 30 °C. The pH of metal solution was adjusted to 6 using a 0.1 M solution of NaOH or a 0.1 M solution of HCl, as previous literature suggests that metal removal increases with an increase in the pH of the solution from 1 to 6, and remained constant at pH 6–7. Increasing the pH beyond 7.0 led to the formation of metal precipitates in the form of hydroxides (Li et al. 2011).

The effects of initial metal concentration on the adsorption of Pb^{2+}, Cu^{2+}, Zn^{2+}, and Ni^{2+} on the PVA/CS/Al_2O_3 adsorbent surface were studied by adding the adsorbents to metal solution with different initial concentration and then shaking the flask for 24 h to ensure that the equilibrium point was reached.

In this study, the metal ion concentration of all experiments was determined using an AA Analysis 200 atomic adsorption spectrometer (AAS), with Pb lamp (283.31 nm), Cu lamp (324.75 nm), Zn lamp (213.86 nm), and Ni lamp (232.00 nm). In addition, all of the experiments were performed in triplicate and the average values were used in the analysis.

Adsorption experiments for the quaternary system

The adsorption characteristics of PVA/CS/Al_2O_3 adsorbents were determined in a quaternary metal mixture. The initial concentration of each metal ion in the mixture was 100 mg/L. The adsorbents (0.1 g) were added to 50 mL of metal mixture at pH 6.0 and the samples were shaken at 100 rpm, 30 °C for 12 h.

The effect of the contact time on the adsorption of Pb^{2+}, Cu^{2+}, Zn^{2+}, and Ni^{2+} in the quaternary system onto the PVA/CS/Al_2O_3 adsorbent surface was studied by allowing the adsorbents to be in contact with the metal mixture and then shaking for 12 h. The samples were collected at predetermined time intervals in each flask separately, and the residual metal concentration was analyzed.

Desorption experiments

The reusability of PVA/CS/Al_2O_3 adsorbents in the adsorption of metal ions was determined in this research. After the adsorbents were used to adsorb metal ions, the adsorbents were regenerated by soaking in a 0.1 M solution of HCl for 24 h. These adsorbents were then washed with deionized water. The regenerated adsorbents were reused in the next adsorption cycle.

Continuous adsorption experiments

The continuous adsorption experiment for the quaternary system was performed via a column experiment. A cylindrical

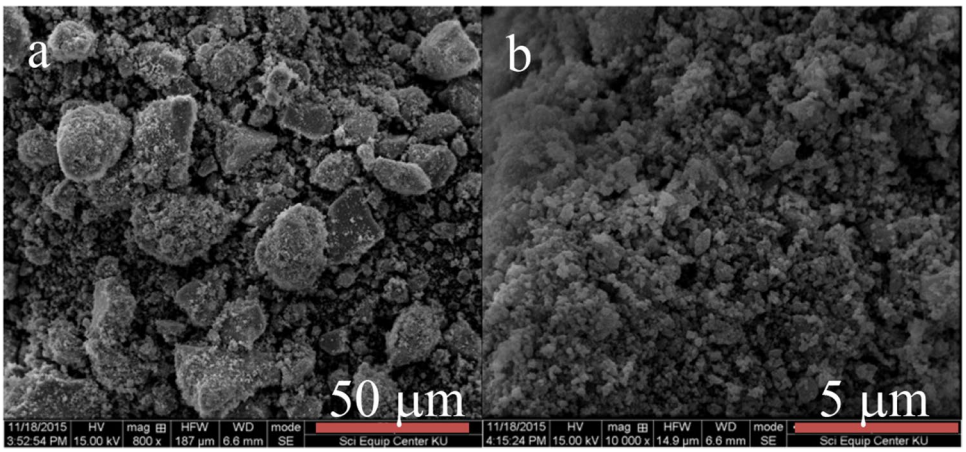

Fig. 1 SEM micrographs of Al_2O_3 particles at magnification of 800× (**a**) and 10,000× (**b**)

column with a diameter of 3.6 cm and a height of 28.4 cm was packed with adsorbents (1 g). The solution level was maintained at 3 cm above the packing and the flow rate was adjusted to 2 mL/min. The samples were collected every 10 min to determine the residual metal concentration.

Results and discussion

In this research, Al_2O_3 particles were synthesized through the sol–gel method as the materials for adsorbent synthesis. The reaction between $Al_2(SO_4)_3$ and NH_4OH resulted in a white powder, which was calcined to obtain Al_2O_3 particles (Sharma et al. 2008). These Al_2O_3 particles were characterized by SEM and XRD techniques, as shown in Figs. 1 and 2, respectively, to confirm the successful synthesis. SEM was performed to observe the morphology of the Al_2O_3 particles (Fig. 1). Following the synthetic process, the images revealed that the Al_2O_3 particles agglomerate due to the strong bonds between primary particles (Furushima et al. 2012). The XRD results show that the spectrum of Al_2O_3 displays a type of α-transition structure, with characteristic peaks located at 2θ of 25.49°, 35.04°, 37.68°, 43.26°, 52.44°, 57.39°, 61.34°, 66.4°, 68.15°, and 76.76° indicated to (012), (104), (110), (113), (024), (116), (122), (124), (030), and (119) crystal planes, respectively (Fig. 2) (Boumaza et al. 2009).

The PVA/CS (mass ratio of 2:2.5) and PVA/CS/Al_2O_3 (mass ratios of 2:2.5:0.25 and 2:2.5:0.50, respectively) were synthesized by mixing PVA, Na-Alg, and $CaCO_3$ in distilled water and stirring at 90 °C. CS and Al_2O_3 were then added to the mixture with different mass ratios. Subsequently, the slurry was added to the 5% $CaCl_2$ in saturated $B(OH)_3$

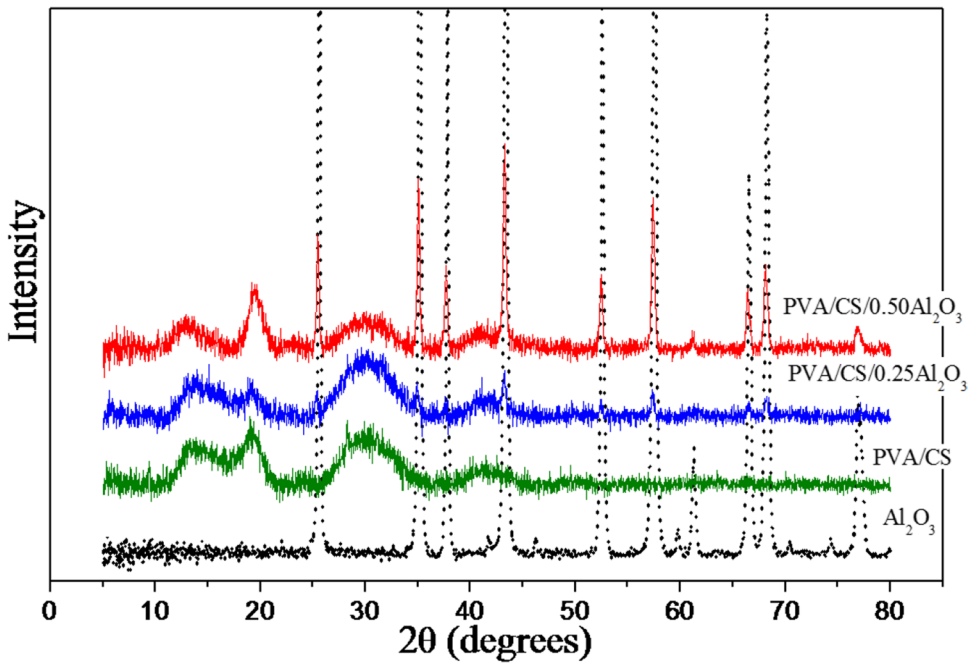

Fig. 2 XRD spectra of Al_2O_3 particles, PVA/CS and PVA/CS/Al_2O_3 adsorbents

solution. This step was required to enhance the stability and the strength of the polymer composites, as calcium (Ca^{2+}) and borate ions ($B(OH)_4^-$) have the ability to cross-link Na-Alg and PVA, respectively. The polymer composite adsorbents were added into a 1 M solution of HCl in order to react with $CaCO_3$, which inserted in the composite adsorbents until gas bubbles were no longer visible in the mixture. This method was used to generate porous materials with suitable properties to be used as adsorbents for the removal of heavy metals.

Morphology of PVA/CS and PVA/CS/Al_2O_3 adsorbents

The morphologies of PVA/CS and PVA/CS/Al_2O_3 adsorbents were studied by SEM. SEM micrographs of the synthesized adsorbents are displayed in Fig. 3. The images reveal the presence of macroporous adsorbents with various sizes, composed of web-like structures due to the reaction between HCl and $CaCO_3$ within the structure of PVA/CS and PVA/CS/Al_2O_3. The results show that PVA/CS/0.50Al_2O_3 has the largest particle size and pore size. Therefore, the results suggest that the incorporation of Al_2O_3 particles into the PVA/CS adsorbents increases the particle size due to the increase in pore size. It may be that the Al_2O_3 particles incorporated into the PVA/CS led to the dilution of the polymer matrix and repulsion between the charges on the Al_2O_3 surface and polymer chain in aqueous solution. This process might affect the size of these adsorbents (Franks and Gan 2007).

In order to determine the percent composition of the PVA/CS/Al_2O_3 adsorbents, EDX technique was introduced. The EDX spectra of PVA/CS/Al_2O_3 adsorbents are shown in Fig. 4, and the weight percent and the atomic percent are shown in Table 1. The results show that the weight percent of aluminum (Al) for PVA/CS/0.25Al_2O_3 is 0.65%, increasing to 2.28% for PVA/CS/0.50Al_2O_3, representing the increase in the amount of Al_2O_3 particles within the adsorbents. In addition, boron (B) and calcium (Ca) were involved in the cross-linking of PVA and Na-Alg during the synthesis, respectively. Thus, the weight percent of B and Ca in PVA/CS/0.25Al_2O_3 were 9.01% and 0.07%, respectively. For PVA/CS/0.50Al_2O_3, these elements increased to 12.79% and 0.08%, respectively. It is likely that the increase of these elements is due to an increase in the number of cross-linked species. This may be due to the space between polymer chains being increased by the presence of Al_2O_3 particles and therefore the cross-linking agents can more easily insert into the space and then react with PVA and Na-Alg (Peña-Reyes et al. 2017).

EDX mapping of the element Al is shown in Fig. 5, representing a good dispersion of Al_2O_3 particles within the PVA/CS matrix. The adsorbents were observed as a homogenous mixture.

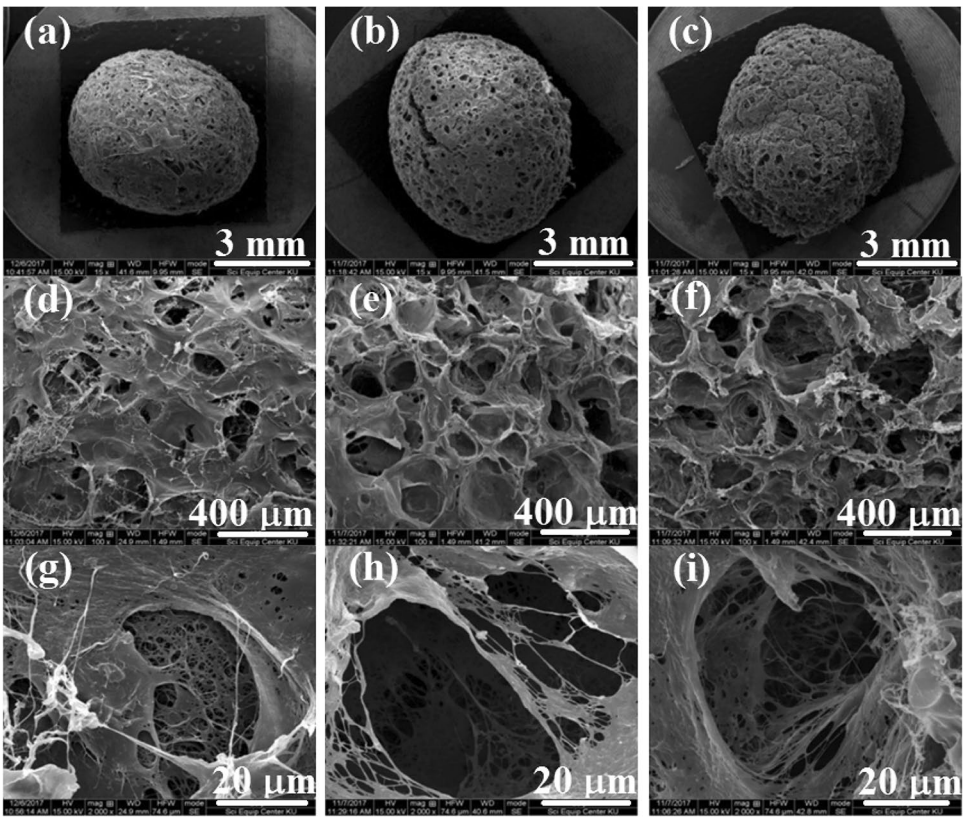

Fig. 3 SEM micrographs of PVA/CS, PVA/CS/0.25Al_2O_3, and PVA/CS/0.50Al_2O_3 at magnification of 15× (**a**–**c**), 100× (**d**–**f**), and 2000× (**g**–**i**), respectively

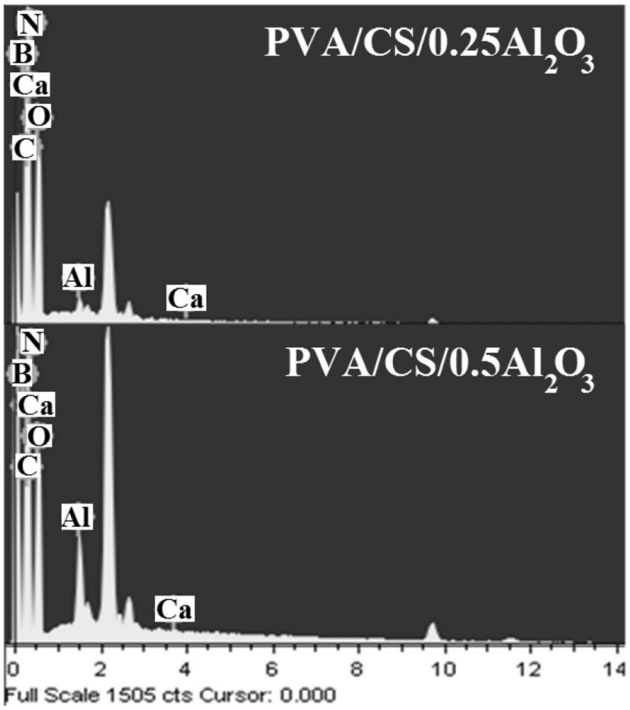

Fig. 4 EDX spectra of PVA/CS/Al_2O_3 adsorbents

X-ray diffraction

In order to investigate the composition of the PVA/CS and PVA/CS/Al_2O_3 adsorbents, the XRD technique was employed. The XRD spectra of PVA/CS and PVA/CS/Al_2O_3 adsorbents with various mass ratios of Al_2O_3 are displayed in Fig. 2. The XRD spectrum of PVA/CS composites exhibited a sharp peak of crystalline phase at 2θ of 19° and broad peaks of semi-crystalline phase around 2θ of 14°, 30°, and 42°. The XRD spectra of PVA/CS/Al_2O_3 adsorbents displayed the PVA/CS peaks (broad and low intensity peaks) and the Al_2O_3 characteristic peaks (sharp peaks at 2θ of 25.49°, 35.04°, 37.68°, 43.26°, 52.44°, 57.39°, 61.34°, 66.4°, 68.15°, and 76.76°), where the intensity increases with increasing amount of Al_2O_3 particles. The sharp diffraction peak of Al_2O_3 particles revealed that these particles had high crystalline nature and were found in the PVA/CS/Al_2O_3 spectra. Furthermore, these results confirmed that the addition of Al_2O_3 particles to the PVA/CS blend in the preparation of PVA/CS/Al_2O_3 adsorbents did not affect the chemical structure.

Brunauer–Emmett–Teller surface analysis (BET)

BET surface analysis was introduced to observe the specific surface area and porosity of the PVA/CS and PVA/CS/Al_2O_3 adsorbents. BET data, such as BET surface area, pore volume, and average pore diameters, are listed in Table 2. The results show that PVA/CS, PVA/CS/0.25Al_2O_3, and PVA/CS/0.50Al_2O_3 adsorbents had surface areas of 11.500, 10.108, and 17.903 m^2/g, and pore volumes of 24.109, 18.145, and 71.873 mm^3/g, while the average pore diameters were 8.263, 7.730, and 14.546 nm, respectively. In the case of PVA/CS/0.25Al_2O_3, the small amount of Al_2O_3 in the composite had a minimal effect on the surface area. However, it was clearly observed that the increase in the amount of Al_2O_3 particles to a mass ratio of 0.50 in the adsorbents led to an increase in surface area, which enhanced the adsorption efficiency due to the increase in contact sites between metal ion and adsorbent surface. PVA/CS/0.50Al_2O_3 showed the best improvement in surface area and pore size.

Thus, the above results suggest that PVA/CS/0.50Al_2O_3 adsorbents exhibit the best properties of the adsorbents studied, such as a larger surface area directly affecting adsorption efficiency. This was a reason why these materials were chosen to use as adsorbents for heavy metals, such as Pb^{2+}, Cu^{2+}, Zn^{2+}, and Ni^{2+}, removal from aqueous solution.

Adsorption experiments for a single system

Effect of initial concentration of heavy metal ions

An important term for the adsorption study was the number of adsorbed species on the surface of adsorbents. This value is related to the concentration of adsorbed species in the solid phase, or the adsorption capacity at equilibrium (Q_e, mg/g), calculated by the following equation:

$$Q_e = \frac{(C_o - C_e)V}{m} \quad (1)$$

where C_o and C_e (mg/L) are the initial and equilibrium concentrations of metal ions in the solution, respectively. V (L) is the volume of the solution and m (g) is the mass of the adsorbents.

Table 1 Composition of PVA/CS/Al_2O_3 adsorbents

Elements	Samples			
	PVA/CS/0.25Al_2O_3		PVA/CS/0.50Al_2O_3	
	Weight (%)	Atom (%)	Weight (%)	Atom (%)
B	9.01	10.93	12.79	15.43
C	52.50	57.31	49.06	53.29
N	4.03	3.77	8.34	7.76
O	33.75	27.66	27.45	22.38
Al	0.65	0.32	2.28	1.10
Ca	0.07	0.02	0.08	0.03

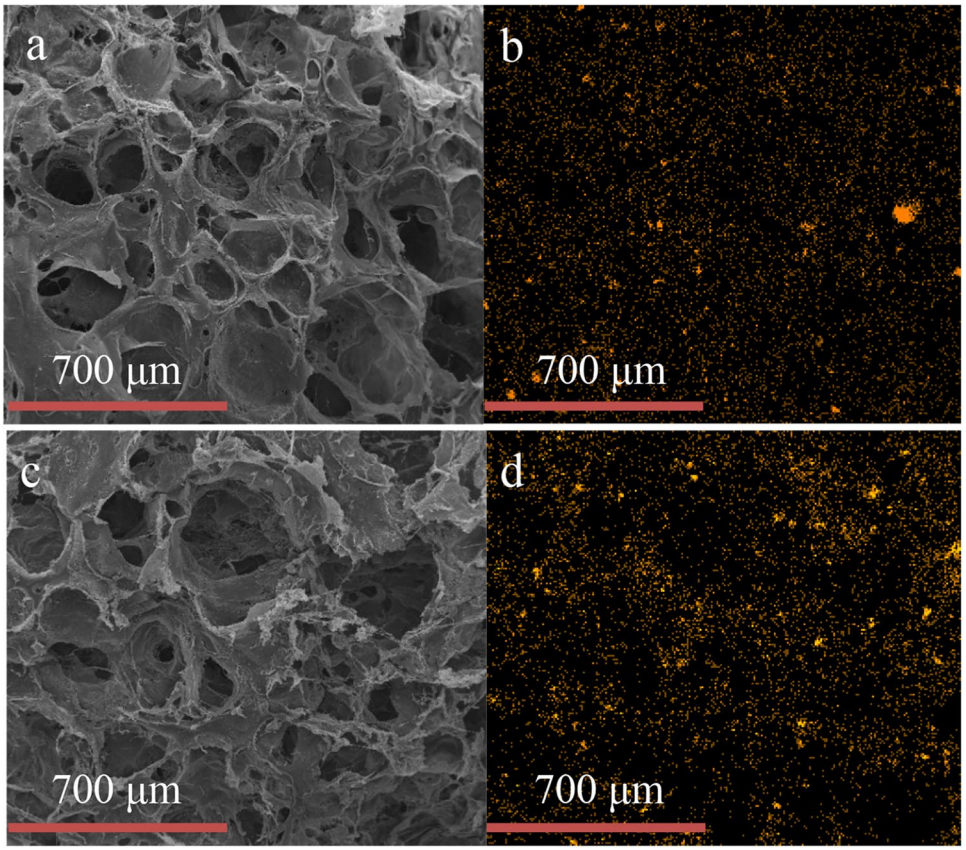

Fig. 5 SEM micrographs and EDX mapping of Al on the surface of PVA/CS/0.25Al_2O_3 (**a**–**b**) and PVA/CS/0.50Al_2O_3 (**c**–**d**) adsorbents

The adsorption of Pb^{2+}, Cu^{2+}, Zn^{2+}, and Ni^{2+} on the PVA/CS/Al_2O_3 adsorbents was studied by the addition of the adsorbents into metal ion solution of different concentration in the range of 100–500 mg/L (ppm) at 30 °C for 24 h. The results are shown in Fig. 6. It was found that the amount of metal ions adsorbed on the surface of PVA/CS/0.50Al_2O_3 adsorbents increased with an increase in initial metal concentration. In addition, the adsorption graph of Pb^{2+}, Cu^{2+}, Zn^{2+}, and Ni^{2+} revealed a steep slope at the low metal concentration which suggested fast metal adsorption. The gradient of the graph slope then slightly decreases at higher concentrations, indicating a slower increase in metal adsorption. The adsorption capacity of Pb^{2+} continuously increased while the adsorption capacity of Cu^{2+}, Zn^{2+}, and Ni^{2+} reached an equilibrium. The maximum adsorption of Pb^{2+}, Cu^{2+}, Zn^{2+}, and Ni^{2+} was determined as 69.48, 45.44, 27.22, and 12.03 mg/g, respectively. This indicated that Pb^{2+} exhibited the strongest affinity for PVA/CS/0.50Al_2O_3 adsorbents, followed by Cu^{2+} and Zn^{2+}, while Ni^{2+} showed the least affinity.

Table 2 Brunauer–Emmett–Teller surface analysis of PVA/CS/Al_2O_3 adsorbents

Samples	BET surface area	Pore volume	Average pore diameter
	m^2/g	mm^3/g	nm
PVA/CS	11.500	24.109	8.263
PVA/CS/0.25Al_2O_3	10.108	18.145	7.730
PVA/CS/0.50Al_2O_3	17.903	71.873	14.546

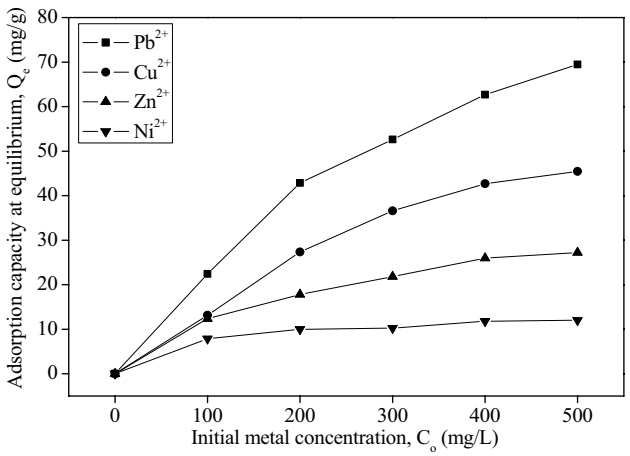

Fig. 6 Effect of initial metal concentration on the adsorption of Pb^{2+}, Cu^{2+}, Zn^{2+}, and $Ni.^{2+}$ on PVA/CS/0.50Al_2O_3 adsorbents

Adsorption isotherm

The adsorption isotherm shows the relationship between the amount of adsorbate left in the solution and the amount of adsorbate adsorbed on the adsorbent surface. In this study, the adsorption isotherm was studied by fitting two different isotherm equations, such as the Langmuir and Freundlich isotherms, to investigate the adsorption behavior of PVA/CS/0.50Al_2O_3 adsorbents in the adsorption of Pb^{2+}, Cu^{2+}, Zn^{2+}, and Ni^{2+}. This could describe the relationship between the concentration of metal ions in the solid phase (metal ion adsorbed onto the adsorbent surface) and in the liquid phase (metal ions remaining in solution).

Langmuir isotherm

The Langmuir isotherm (Langmuir 1916, Zhou et al. 2018, Zhou et al. 2015) describes the equilibrium between adsorbate and adsorbent systems. The adsorbate adsorption is limited to monolayer adsorption (one molecular layer) on a homogenous surface. There is no lateral interaction between adjacently adsorbed molecules and a single molecule occupies a single binding site. The binding sites have equal affinity and energy. The Langmuir equation is given as Eq. (2) below:

$$\frac{C_e}{Q_e} = \frac{1}{K_L Q_{max}} + \frac{C_e}{Q_{max}} \tag{2}$$

where Q_e (mg/g) and C_e (mg/L) are the adsorption capacity of the metal on the adsorbent surface at equilibrium and the residue concentration of metal in solution (equilibrium concentration of metal on solid and liquid phase), respectively. Q_{max} (mg/g) and K_L (L/mg) are the Langmuir constants related to saturated monolayer adsorption capacity and binding energy of the adsorption system, respectively.

Freundlich isotherm

The Freundlich isotherm (Freundlich 1906), an empirical adsorption model, assumes a multilayer adsorption of metal ions onto a heterogeneous surface. The amount of adsorbate that is adsorbed onto the adsorbent surface increases infinitely with the increase in adsorbate concentration. The linearized Freundlich equation is given as Eq. (3) below:

$$\ln Q_e = \ln K_f + \frac{1}{n}\ln C_e \tag{3}$$

where Q_e (mg/g) is the adsorption capacity of metal on the adsorbent surface at equilibrium and C_e (mg/L) is the residue concentration of metal in solution (equilibrium concentration of metal on solid and liquid phase, respectively). K_f and n are the Freundlich constant related to adsorption capacity and intensity, respectively.

The Langmuir and Freundlich constants, and the correlation coefficients (R^2) are listed in Table 3. It was observed that the Freundlich model showed the highest R^2 value. This indicates that the equilibrium data obtained from adsorption of Pb^{2+}, Cu^{2+}, Zn^{2+}, and Ni^{2+} on the PVA/CS/0.50Al_2O_3 adsorbents is a good fit for the Freundlich isotherm model. The adsorption characteristic occurred for heterogeneous interactions between the metal ions and PVA/CS/0.50Al_2O_3 adsorbents. The n constant, which represents the amount of adsorption, was greater than 1, indicating good adsorption at high concentrations.

FTIR analysis

The adsorption mechanism of PVA/CS/0.50Al_2O_3, before and after metal adsorption, was investigated by FTIR spectroscopy, and the spectra are shown in Fig. 7.

In the case of PVA/CS/0.50Al_2O_3 before adsorption, PVA showed a characteristic broad band between 3000 and 3600 cm^{-1} and another bending vibration at $\upsilon = 1647$ cm^{-1}, which refers to –OH groups involved in intramolecular and intermolecular hydrogen bonding. The bands at 2905 cm^{-1} and at 1417 cm^{-1} were stretching and bending vibrations of $–CH_2$ and CH–O–H, respectively. Moreover, characteristic saccharine bands at 1072 cm^{-1} and 947 cm^{-1}, as well as the band between 3000 and 3600 cm^{-1} for $–NH_2$ and –OH groups, were good evidence for the CS structure. The two characteristic peaks of Al_2O_3 at $\upsilon = 634$ cm^{-1} and 562 cm^{-1} were evidence for the incorporation of Al_2O_3 molecules into the polymer matrix. However, there was a clear increase in the intensity of these bands for the PVA/CS/0.50Al_2O_3 following metal adsorption, which is attributed to the interaction with metal ions. Therefore, the shift and the intensity increase

Table 3 Isotherm constants for adsorption based on the Langmuir isotherm and Freundlich isotherm

Kinetics parameters	Pb^{2+}	Cu^{2+}	Zn^{2+}	Ni^{2+}
Q_{exp} (mg/g)	69.48	45.44	27.22	12.03
Langmuir isotherm				
Q_{max} (mg/g)	-5.56×10^{4}	1250.00	2304.15	303.03
K_L (L/mg)	-8.92×10^{-6}	4.02×10^{-4}	2.16×10^{-4}	1.69×10^{-3}
R^2	0.001378	0.1081	0.5299	0.9645
Freundlich isotherm				
K_f (mg/g)	0.495	0.536	0.509	0.546
n	0.999	1.023	1.009	1.033
R^2	1.0000	0.9964	0.9999	0.9999

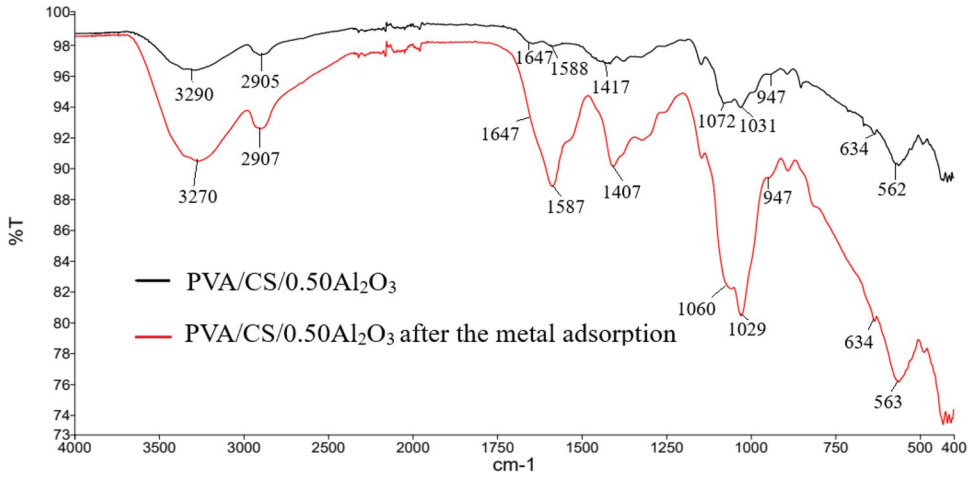

Fig. 7 FTIR spectra of PVA/CS/0.50Al_2O_3, before and after metal adsorption

in all bands were the interaction between the adsorbent and metal ions.

The mechanism of adsorption might occur through the electrostatic interactions between the positive charge of the metal ions and the negative charge of lone pair electrons on the binding sites of adsorbents resulting in the formation of metal complexes. In general, PVA and chitosan contain electron donating groups, such as hydroxyl groups (–OH) and amine groups ($–NH_2$), while Al_2O_3 contains many pairs of electrons belonging to oxygen atoms and hydroxyl groups on its surface. The affinities of the different metal ions can be explained on the basis of their electronegativity and hydration energy. The order of electronegativity is as follows: $Cu^{2+} > Ni^{2+} > Pb^{2+} > Zn^{2+}$ (Arias et al. 2002). Considering only this parameter, the results suggest that Cu^{2+} exhibits a strong attraction to the lone pairs present on binding sites, forming stable complexes. However, hydration energy is also an important parameter for explaining the result, because this is involved in the replacement of water ligands with hydroxyl groups. The hydration energy was observed in the following order: $Ni^{2+} > Zn^{2+} > Cu^{2+} > Pb^{2+}$ (Liu et al. 2008; Ricordel et al. 2001). Thus, Pb^{2+} might attach to the binding sites of adsorbents more easily. In addition, the hard-soft/acid–base phenomenon between metal ions and the binding sites of adsorbents was another factor for consideration. Previous literature shows that the modified 1-nitroso-2-naphthol alumina in neutral phase selectively adsorbed Pb^{2+} over Cu^{2+} from wastewater at low metal ion concentrations (mg/L) (Mahmoud et al. 2010).

Adsorption experiments for a quaternary system

In the single system, there was no competition between cationic adsorbates and therefore their adsorption characteristic could be easily determined. However, a system consisting of different metal species under the same condition was more interesting to investigate, which would consider the adsorption behavior of each metal ion on the adsorbents. Therefore, an adsorption experiment using PVA/CS/0.50Al_2O_3 was studied for the quaternary system.

The PVA/CS/0.50Al_2O_3 adsorbents were introduced and allowed to contact a mixture of Pb^{2+}, Cu^{2+}, Zn^{2+}, and Ni^{2+} ions, with a concentration of 100 mg/L of each metal ion, for 12 h to reach equilibrium. The adsorption capacity at equilibrium obtained experimentally (Q_{exp}, mg/g) for the metal ions is listed in Table 4. The adsorption capacity values at equilibrium of Pb^{2+}, Cu^{2+}, Zn^{2+}, and Ni^{2+} were 12.50, 7.49, 6.93, and 6.75, respectively. The affinity of each type of metal ion was in the same order: $Pb^{2+} > Cu^{2+} > Zn^{2+} > Ni^{2+}$. Thus, it is observed that the dominant adsorption characteristic among these heavy metal ions was found in both of the single and multiple systems.

The effect of contact time

The kinetic study of the adsorption experiment for the quaternary system was performed by studying the effect of contact time on the adsorption of Pb^{2+}, Cu^{2+}, Zn^{2+}, and Ni^{2+} onto the PVA/CS/0.50Al_2O_3 adsorbents. The kinetic curves are shown in Fig. 8. These curves illustrate the relationship between contact time and adsorption capacity (Q_t, mg/g). The results show that adsorption capacity increased with the increase in contact time. The adsorption capacity of Zn^{2+} reached equilibrium at 120 min, while the others were still increasing at 720 min.

Table 4 Adsorption capacity of a quaternary system (Pb^{2+}, Cu^{2+}, Zn^{2+}, and $Ni.^{2+}$) on PVA/CS/0.50Al_2O_3 adsorbents

Adsorption	Pb^{2+}	Cu^{2+}	Zn^{2+}	Ni^{2+}
Q_{exp} (mg/g)	12.50 ± 1.80	7.49 ± 1.55	6.93 ± 0.47	6.75 ± 2.03

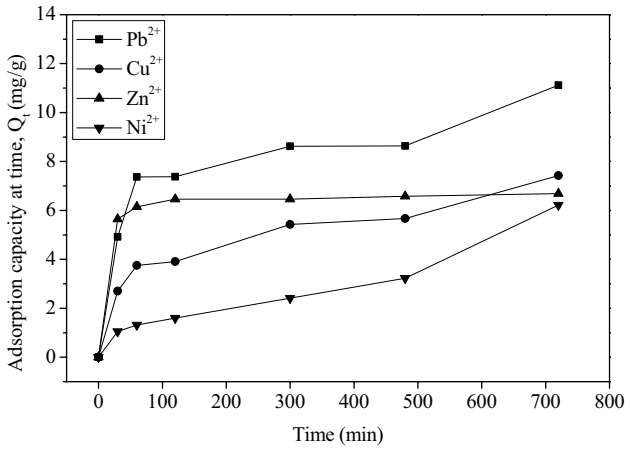

Fig. 8 Effect of contact time on the adsorption of Pb^{2+}, Cu^{2+}, Zn^{2+}, and $Ni.^{2+}$ onto PVA/CS/0.50Al_2O_3 adsorbents

Adsorption kinetics

The adsorption behavior of the adsorption of Pb^{2+}, Cu^{2+}, Zn^{2+}, and Ni^{2+} onto PVA/CS/0.50Al_2O_3 adsorbents was investigated. Adsorption kinetic models, such as pseudo-first order and pseudo-second order, were used to fit the data obtained from the kinetic experiment of the quaternary system, including the adsorption capacity as a function of time.

A pseudo-first-order model assumes the adsorption of one adsorbate molecule on one active site of the adsorbent surface (Ibrahim et al. 2019; Khan et al. 2015).

The pseudo-first-order equation is given as Eq. (4) below:

$$\ln\left(Q_e - Q_t\right) = \ln Q_e - K_1 t \tag{4}$$

where Q_e (mg/g) and Q_t (mg/g) are the adsorption capacity at equilibrium and at predetermined time t (min), respectively. K_1 is the first-order rate constant (1/min).

A pseudo-second-order model has the assumption that the adsorption capacity is dependent on the number of active sites on the adsorbent surface. The pseudo-second-order equation (Ho and McKay 1998) is expressed as Eq. (5):

$$\frac{t}{Q_t} = \frac{1}{K_2 Q_e^2} + \frac{t}{Q_e} \tag{5}$$

where K_2 (g/(mg min)) is the second-order rate constant.

The kinetic constants obtained from pseudo-first-order and pseudo-second-order models are listed in Table 5. The results for Pb^{2+}, Cu^{2+}, and Zn^{2+} show that the correlation coefficient (R^2) obtained from the pseudo-second-order model is higher than that obtained from the pseudo-first-order model. This indicates that the pseudo-second-order kinetic model fitted the experimental data better than the pseudo-first-order kinetic model. Thus, we can conclude that the adsorption kinetics of Pb^{2+}, Cu^{2+}, and Zn^{2+} behave according to pseudo-second-order kinetics. The theoretical adsorption capacity values calculated from the equation were close to the experimental values. Moreover, the adsorption rate of Zn^{2+} was the fastest, followed by Pb^{2+}, while Cu^{2+} displayed the slowest rate. On the other hand, Ni^{2+} exhibited adsorption behavior expected for a pseudo-first-order model more than a pseudo-second-order model, as shown by the higher correlation coefficient. In the early stages, the adsorption capacity increased with adsorption rate but then increased later. The reason might be related to the affinity of Ni^{2+}. This ion showed the lowest adsorption efficiency and the effect of a competitive system of multiple adsorbates with a limited number of active sites may have controlled the adsorption rate.

Table 5 Kinetic parameters obtained from the kinetic equation based on the pseudo-first-order and pseudo-second-order models

Kinetic parameters	Pb^{2+}	Cu^{2+}	Zn^{2+}	Ni^{2+}
Q_{exp} (mg/g)	12.50	7.20	6.93	6.75
Pseudo-first-order				
Q_e (mg/g)	8.24	7.21	1.58	7.43
K_1 (min^{-1})	0.0023	0.0053	0.0031	0.0029
R^2	0.8318	0.8393	0.5526	0.8063
Pseudo-second-order				
Q_e (mg/g)	11.07	7.71	6.72	7.22
K_2 (g/(mg min))	0.0016	0.0014	0.0217	0.0004
R^2	0.9696	0.9624	0.9998	0.6308

Desorption

Reusability was the most important factor for deciding if the novel adsorbents were an improvement on the previous ones. This property makes the adsorption process more economical and feasible. In addition, the regeneration process should not be complicated. Thus, the reusability of PVA/CS/0.50Al_2O_3 adsorbents was investigated. In the previous literature, many desorbing agents such as distilled water, HCl, and EDTA at various concentrations were used to regenerate adsorbents. The results suggest that a 0.1 M solution of HCl provides the optimal performance for the desorption of various metal ions (Li et al. 2011). Thus, the used adsorbents were regenerated by soaking in a 0.1 M solution HCl and shaking for 24 h. The regenerated adsorbents were then used for next adsorption cycle and this cycle was repeated twice. The results are shown in Fig. 9 and the percentage adsorption of each cycle is listed in Table 6.

The adsorption capacities of Pb^{2+}, Cu^{2+}, Zn^{2+}, and Ni^{2+} onto the PVA/CS/0.50Al_2O_3 adsorbents decreased with additional adsorption cycles. The percentage adsorption of Pb^{2+}, Cu^{2+}, Zn^{2+}, and Ni^{2+} in the first reuse was 92.59%,

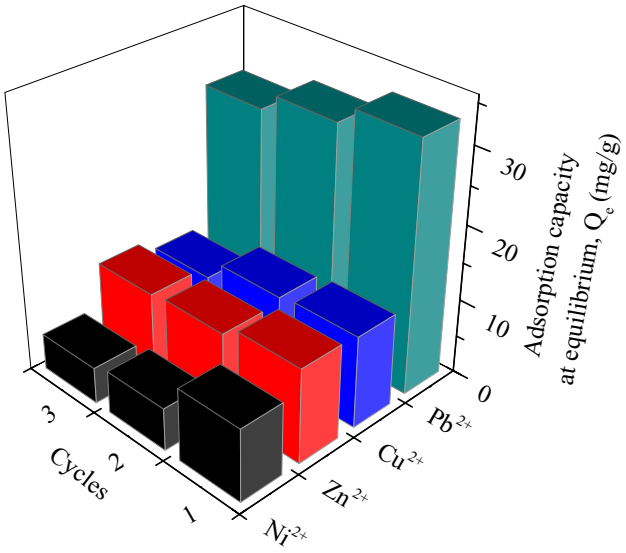

Fig. 9 Adsorption capacities of PVA/CS/0.50Al_2O_3 adsorbents after adsorption–desorption processes

Table 6 The percentage adsorption of Pb^{2+}, Cu^{2+}, Zn^{2+}, and $Ni.^{2+}$ on the PVA/CS/0.50Al_2O_3 adsorbents in the first and second reuse

%Adsorption	Pb^{2+}	Cu^{2+}	Zn^{2+}	Ni^{2+}
First reuse	92.59	96.30	88.10	58.33
Second reuse	85.19	85.19	84.92	49.79

96.30%, 88.10%, and 58.33%, respectively, which decreased to 85.19%, 85.19%, 84.92%, and 49.79%, respectively, in the second reuse. The results indicated that Pb^{2+}, Cu^{2+}, and Zn^{2+} could be desorbed using 0.1 M HCl efficiently, while the desorption of Ni^{2+} with HCl was inefficient. However, PVA/CS/0.50Al_2O_3 adsorbents could be regenerated for reuse and this ability would decrease the operational costs of industrial application. Thus, the PVA/CS/0.50Al_2O_3 materials are efficient adsorbents for economic metal ion removal.

Continuous adsorption experiments

The preliminary column experiment was designed for further use of the PVA/CS/0.50Al_2O_3 adsorbents for metal ion removal on an industrial scale. In the experiment, the solution of metal ions, with flow rate of 2 mL/min, was passed through the column packed with PVA/CS/0.50Al_2O_3 adsorbents as a fixed bed, and the samples were collected at a predetermined time, in order to investigate the residual concentration of the metal ions. This experiment was performed for 12 h, assuming that the column could be used successfully for metal ion removal for infinite time. The breakthrough curves of continuous adsorption are displayed in Fig. 10.

The total removal amount (Q_{total}) could be evaluated according to Eq. (6) (de Freitas et al. 2018)

$$Q_{total} = \frac{C_o \bullet G}{1000 \bullet m} \int_0^t \left(1 - \frac{C_t}{C_o}\right) dt \tag{6}$$

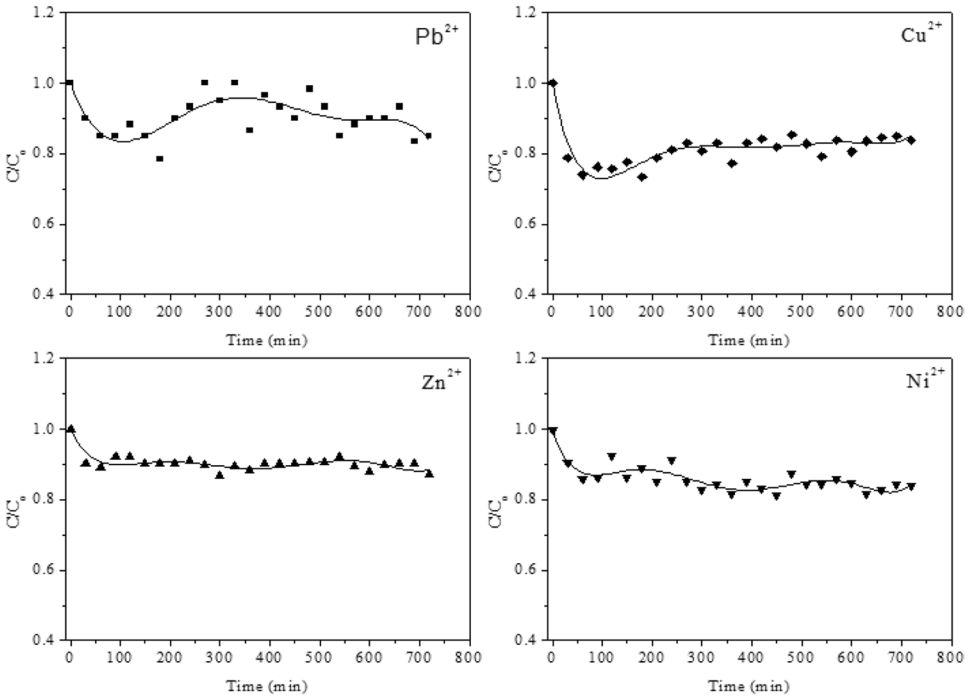

Fig. 10 Breakthrough curves of the column experiment for continuous adsorption of Pb^{2+}, Cu^{2+}, Zn^{2+}, and $Ni.^{2+}$ by PVA/CS/0.50Al_2O_3 adsorbents as a fixed bed

Table 7 Total amount of removed metal ions in the continuous adsorption experiment

Continuous adsorption	Pb^{2+}	Cu^{2+}	Zn^{2+}	Ni^{2+}
Q_{total} (mg/g)	20.62	40.32	17.46	27.05

where G (mL/min) is the flow rate of metal solution; C_o and C_t (mg/L) are the inlet metal concentration and outlet concentration at time t.

The breakthrough curves indicated that the outlet concentrations of metal ions after 12 h of sampling were still lower than that of the inlet concentration. These results related to kinetic adsorption experiments showed that the adsorption rate of Pb^{2+}, Cu^{2+}, Zn^{2+}, and Ni^{2+} on the PVA/CS/0.50Al_2O_3 adsorbents was very slow. However, the adsorption of Cu^{2+} predominated in the selective competition for static column adsorption. The Q_{total} values of each metal ion are shown in Table 7, and these follow the order: $Cu^{2+} > Ni^{2+} > Pb^{2+} > Zn^{2+}$. This suggests that the electronegativity and charge density lead to strong attractions in the negative binding sites. Moreover, there was less metal adsorption by the column because no external force was added to enhance the freely mobilized metal ions in the mixture, and the mixed solution might have passed through the column too quickly to allow strong electrostatic interactions between the metal ions and the adsorbent surface.

Conclusion

The PVA/CS, PVA/CS/0.25Al_2O_3, and PVA/CS/0.50Al_2O_3 composite adsorbents were synthesized and characterized. The adsorption of Pb^{2+}, Cu^{2+}, Zn^{2+}, and Ni^{2+} onto these adsorbents was investigated, from aqueous solution. The PVA/CS/0.50Al_2O_3 adsorbents exhibited good chemical stability and excellent adsorption ability from Pb^{2+}, Cu^{2+}, Zn^{2+}, and Ni^{2+} solutions. Important factors affecting the adsorption, such as initial concentration and contact time, were studied. The Freundlich isotherm was applied to explain the adsorption behavior of PVA/CS/0.50Al_2O_3 for Pb^{2+}, Cu^{2+}, Zn^{2+}, and Ni^{2+} removal. The kinetic results suggested that the adsorption kinetic behavior of Pb^{2+}, Cu^{2+}, and Zn^{2+} followed a pseudo-second-order model. However, Ni^{2+} exhibited pseudo-first-order model adsorption behavior. Competitive adsorption was studied in quaternary metal systems. It was confirmed that PVA/CS/0.50Al_2O_3 displayed the highest selectivity towards Pb^{2+} over the other metal ions. In addition, the re-adsorption capacities were studied. It was found that the adsorbents could attain a high percent of the initial adsorption values after many cycles of adsorption–desorption operations. This confirmed the reusability of the PVA/CS/0.50Al_2O_3 adsorbents. Overall, it can be concluded that PVA/CS/0.50Al_2O_3 had the greatest adsorption capabilities for heavy metal removal from aqueous solution, and it was also an eco-friendly and reusable adsorbent. Thus, this material is a good choice to apply to metal removal from wastewater, owing to its high adsorption and selectivity, low cost, easy preparation, uncomplicated separation, and excellent reusability.

Acknowledgements This research is supported in part by the Graduate Program Scholarship from the Graduate School, Kasetsart University. The authors are sincerely thankful to the Center of Excellence-Oil Palm, Department of Chemistry, Faculty of Science, the Graduate School and Kasetsart University Research and Development Institute (KURDI), Kasetsart University, for financial support. In addition, the authors wish to thank the Department of Chemistry, Faculty of Science, Kasetsart University, for providing the devices.

Author contribution All authors contributed to the study conception and design. Material preparation, data collection, and analysis were performed by Methus Charoenchai and Siree Tangbunsuk. The first draft of the manuscript was written by Methus Charoenchai and Siree Tangbunsuk, and all authors commented on previous versions of the manuscript. All authors read and approved the final manuscript.

Funding This work was supported by Kasetsart University Research and Development Institute (KURDI), Kasetsart University. The author Methus Charoenchai has received research support from Graduate Program Scholarship from the Graduate School, Kasetsart University.

Declarations

Ethics approval This study did not involve any human subjects and/or animals.

Consent to participate Not applicable.

Consent for publication Not applicable.

Competing interests The authors declare no competing interests.

References

Arias M, Barral MT, Mejuto JC (2002) Enhancement of copper and cadmium adsorption on kaolin by the presence of humic acids. Chemosphere 48:1081–1088. https://doi.org/10.1016/S0045-6535(02)00169-8

Boumaza A, Favaro L, Lédion J, Sattonnay G, Brubach JB, Berthet P, Huntz AM, Roy P, Tétot R (2009) Transition alumina phases induced by heat treatment of boehmite: An X-ray diffraction and infrared spectroscopy study. J Solid State Chem 182:1171–1176. https://doi.org/10.1016/j.jssc.2009.02.006

de Freitas ED, de Almeida HJ, de Almeida Neto AF, Vieira MGA (2018) Continuous adsorption of silver and copper by Verdelodo bentonite in a fixed bed flow-through column. J Clean Prod 171:613–621. https://doi.org/10.1016/j.jclepro.2017.10.036

Franks GV, Gan Y (2007) Charging behavior at the alumina–water interface and implications for ceramic processing. J Am Ceram Soc 90:3373–3388. https://doi.org/10.1111/j.1551-2916.2007.02013.x

Freundlich H (1906) Over the adsorption in solution. J Phys Chem 57A:385–471

Furushima R, Tanaka S, Xue C, Uematsu K (2012) Quantitative analysis of de-aggregation behavior in alumina suspension by beads milling. Powder Technol 217:619–623. https://doi.org/10.1016/j.powtec.2011.11.038

Futalan CM, Kan C-C, Dalida ML, Hsien K-J, Pascua C, Wan M-W (2011) Comparative and competitive adsorption of copper, lead, and nickel using chitosan immobilized on bentonite. Carbohyd Polym 83:528–536. https://doi.org/10.1016/j.carbpol.2010.08.013

Ho YS, McKay G (1998) Kinetic models for the sorption of dye from aqueous solution by wood. Process Saf Environ 76:183–191. https://doi.org/10.1205/095758298529326

Hua M, Zhang S, Pan B, Zhang W, Lv L, Zhang Q (2012) Heavy metal removal from water/wastewater by nanosized metal oxides: a review. J Hazard Mater 211–212:317–331. https://doi.org/10.1016/j.jhazmat.2011.10.016

Ibrahim AG, Saleh AS, Elsharma EM, Metwally E, Siyam T (2019) Chitosan-g-maleic acid for effective removal of copper and nickel ions from their solutions. Int J Biol Macromol 121:1287–1294. https://doi.org/10.1016/j.ijbiomac.2018.10.107

Khan TA, Khan EA, Shahjahan (2015) Removal of basic dyes from aqueous solution by adsorption onto binary iron-manganese oxide coated kaolinite: non-linear isotherm and kinetics modeling. Appl. Clay Sci 107:70–77. https://doi.org/10.1016/j.clay.2015.01.005

Langmuir I (1916) The constitution and fundamental properties of solids and liquids Part I. solids. J Am Chem Soc 38:2221–2295. https://doi.org/10.1021/ja02268a002

Li X, Li Y, Ye Z (2011) Preparation of macroporous bead adsorbents based on poly(vinyl alcohol)/chitosan and their adsorption properties for heavy metals from aqueous solution. Chem Eng J 178:60–68. https://doi.org/10.1016/j.cej.2011.10.012

Liu C, Bai R, San Ly Q (2008) Selective removal of copper and lead ions by diethylenetriamine-functionalized adsorbent: Behaviors and mechanisms. Water Res 42:1511–1522. https://doi.org/10.1016/j.watres.2007.10.031

Mahmoud ME, Osman MM, Hafez OF, Elmelegy E (2010) Removal and preconcentration of lead (II), copper (II), chromium (III) and iron (III) from wastewaters by surface developed alumina adsorbents with immobilized 1-nitroso-2-naphthol. J Hazard Mater 173:349–357. https://doi.org/10.1016/j.jhazmat.2009.08.089

Mishra PC, Patel RK (2009) Removal of lead and zinc ions from water by low cost adsorbents. J Hazard Mater 168:319–325. https://doi.org/10.1016/j.jhazmat.2009.02.026

Peña-Reyes VL, Marin-Bustamante MQ, Manzo-Robledo A, Chanona-Pérez JJ, Cásarez-Santiago RG, Suarez-Najera E (2017) Effect of crosslinking of alginate / pva and chitosan / pva, reinforced with cellulose nanoparticles obtained from agave Atrovirens karw. Procedia Eng 200:434–439. https://doi.org/10.1016/j.proeng.2017.07.061

Rahmani A, Mousavi HZ, Fazli M (2010) Effect of nanostructure alumina on adsorption of heavy metals. Desalination 253:94–100. https://doi.org/10.1016/j.desal.2009.11.027

Ricordel S, Taha S, Cisse I, Dorange G (2001) Heavy metals removal by adsorption onto peanut husks carbon: characterization, kinetic study and modeling. Sep Purif Technol 24:389–401. https://doi.org/10.1016/S1383-5866(01)00139-3

Sharma YC, Srivastava V, Upadhyay SN, Weng CH (2008) Alumina nanoparticles for the removal of Ni(II) from aqueous solutions. Ind Eng Chem Res 47:8095–8100. https://doi.org/10.1021/ie800831v

Sharma YC, Srivastava V, Singh V, Kaul SN, Weng CH (2009) Nano-adsorbents for the removal of metallic pollutants from water and Wastewater. Environ. Technol 30:583–609. https://doi.org/10.1080/09593330902838080

Zhou Y, Zhang R, Gu X, Lu J (2015) Adsorption of divalent heavy metal ions from aqueous solution by citric acid modified pine sawdust. Separ Sci Technol 50:245–252. https://doi.org/10.1080/01496395.2014.956223

Zhou Y, Hu Y, Huang W, Cheng G, Cui C, Lu J (2018) A novel amphoteric β-cyclodextrin-based adsorbent for simultaneous removal of cationic/anionic dyes and bisphenol A. Chem Eng J 341:47–57. https://doi.org/10.1016/j.cej.2018.01.155

Zhou Q, Yang N, Li Y, Ren B, Ding X, Bian H, Yao X (2020) Total concentrations and sources of heavy metal pollution in global river and lake water bodies from 1972 to 2017. Glob Ecol Conserv 22:e00925. https://doi.org/10.1016/j.gecco.2020.e00925